

Effect of impeller speed on properties of quiescent zone and entrainment in mechanical flotation cells

S. Razmjooei, M. Abdollahy* and M.R. Khalesi

Department of Mining Engineering, Faculty of Engineering & Technology, Tarbiat Modares University, Tehran, Iran

Received 6 January 2018; received in revised form 14 February 2018; accepted 15 February 2018

*Corresponding author: minmabd@modares.ac.ir (M. Abdollahy).

Abstract

Flotation process in mechanical cells is carried out in highly turbulent conditions. In this work, the impact of impeller speed on four characteristics of the quiescent zone, i.e. zone height, turbulence, solid percentage, and gas holdup, and their relationship with the entrainment is investigated, and it is shown why at a higher impeller speed, entrainment is not significant. The height of the quiescent zone and its turbulence are measured using a piezoelectric sensor, while an electrical conductivity sensor measures the gas hold-up. A peristaltic pump is applied to take samples from the pulp to measure the solid percentage. The results obtained showed that with increase in the impeller speed from 750 to 1100 rpm, the entrainment value changed from 2.01% to 5.69%. However, the variations in entrainment were not significant at speeds higher than 1100 rpm. It was found that the height of the quiescent zone was independent from the impeller speed, while raising the impeller speed, as long as the solid percentage, turbulence, and gas hold-up are increased, caused a drastic increase in entrainment. Despite the increase in the solid percentage and turbulence, the gas hold-up decreased at impeller speeds higher than 1100 rpm due to the variation in the bubble distribution pattern, so the entrainment raised with a smaller slope. Finally, a model is presented for the entrainment as a function of the three correlated variables using the Ridge regression. The entrainment is then correlated to the impeller speed, explaining the contradictory results from the literature on the effect of impeller speed on the entrainment.

Keywords: *Impeller Speed, Turbulence, Quiescent Zone, Entrainment, Mechanical Flotation Cell.*

1. Introduction

Entrainment occurs simultaneously with true flotation. Unlike true flotation, entrainment is not chemically selective, and it occurs by no direct attachment of particles to bubbles. Therefore, both the valuable and gangue minerals may experience entrainment. Since this process is non-selective, it would have a detrimental effect on the grade of the concentrate [1]. Transport of the entrained particles to the froth phase can be due to the turbulence caused by the impeller (mechanical entrainment) or due to their particle size as well as the density by three mechanisms including the Boundary Layer, Bubble Wake, and Bubble Swarm mechanisms (hydraulic entrainment) [2]. In the Boundary Layer Theory, mineral particles are transported to the froth phase in the bubble

lamella, i.e. the thin hydrodynamic layer of water surrounding the bubble, while in the Bubble Wake Theory, water including the mineral particles is transported to the froth phase in the wake of an ascending bubble [1].

In the bubble swarm theory, water is pushed up into the froth region by ascending swarms of gas bubbles [1]. In a mechanical flotation cell, the formation of three specific hydrodynamic zones including the turbulent, quiescent, and froth zone is essential for an effective flotation [3]. The turbulent zone affects solids suspension, gas dispersion, and bubble-particle interactions. Quiescent zone helps to reduce the probability of gangue mineral recovery caused by possible mechanical entrainment [4]. Therefore, a better

understanding of the properties of this zone is essential to reduce the entrainment.

The factors affecting entrainment including water recovery, particle properties (size, shape, and density), rheological properties of pulp, retention time, and froth height have been studied by several researchers [1-3, 5, 6]. Besides, it has been observed that the turbulence induced by the impeller leads to entrainment [5]. An early research work by Schubert showed that the mechanical and hydraulic entrainments decreased by reducing the turbulence in the quiescent zone [5]. Moreover, Cilek, Akdemir, and Sönmez showed that entrainment increased with increasing impeller speed [7, 8]. To the contrary, in a later research work by Wang et al., it was shown that the impeller speed and its interaction with other factors did not have a significant impact on the entrainment, compared to factors such as air flow, froth height, and particle size [9]. Moreover, in another study, Yang et al. showed that the

entrainment was enhanced by increasing the impeller speed; however, after a while, the variations in the entrainment values in the various speeds of impeller became insignificant [10]. In comparison with the other variables of the quiescent zone, the effect of turbulence on entrainment has been far less investigated. Hence, in the present work, the effect of impeller speed (as a factor creating turbulence) on the properties of the quiescent zone and its relation with entrainment have been investigated.

2. Material and methods

In order to study the effect of impeller-induced turbulence on the properties of the quiescent zone including the height, solid percentage, gas hold-up, and turbulence, and its relation with entrainment, a number of experiments were performed using a 9-liter mechanical flotation cell. Figure 1 schematically demonstrates the positions where these variables were measured.

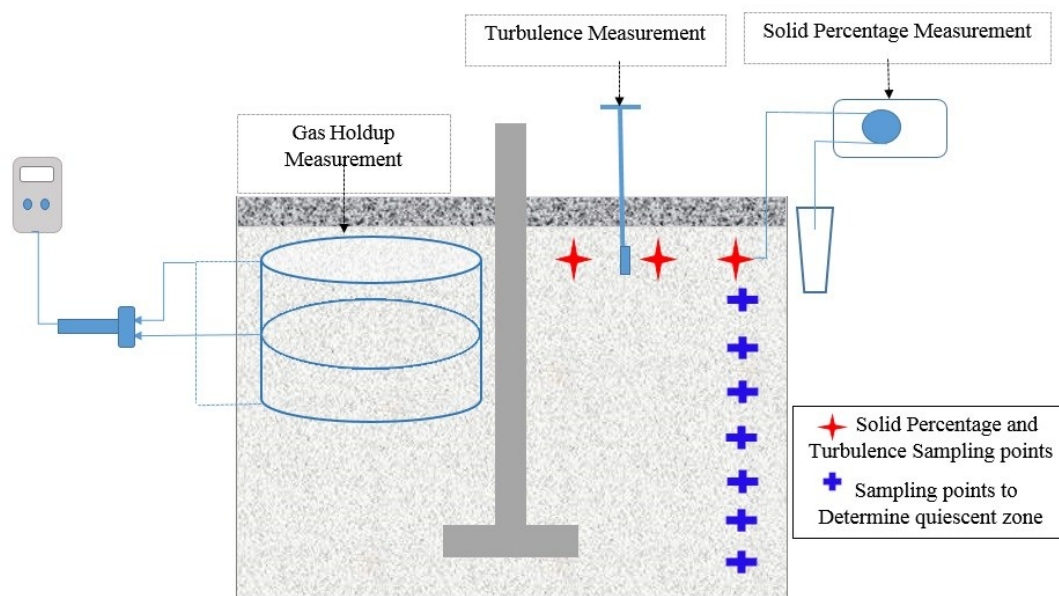


Figure 1. Schematic representation of experimental equipment.

2.1. Materials

Ultrapure quartz (99.99% pure) ground in a ceramic mill to -50 micron was used in the experiments. 30 ppm MIBC (Isfahan Copolymer Co.) (higher than the critical coalescence concentration) and 500 ppm sodium silicate (Merck Co.) were used as the frother and the dispersant, respectively.

2.2. Method

2.2.1. Flotation experiments

The Trahar's method was used to measure the entrainment (mechanical and hydraulic) [11].

Therefore, the flotation experiments were conducted without a collector. The ratio of mass of solids transported to the concentrate to the solids in feed was considered as the recovery by entrainment.

During the floatation tests, all the operating conditions were kept constant, and only the impeller speed was manipulated. Firstly, sodium silicate was added to a pulp of 8% solid percentage. Next, the frother was added, and 3.5 l/min of air was sparged. The froth was scraped every 2 seconds automatically afterward. The making water was added to the cell with the same

concentration of the pulp via a peristaltic pump in order to maintain the froth-pulp interface level constant during the experiments.

2.2.2. Determining quiescent zone

The method presented by Tabosa et al. was used to determine the turbulent zone as well as the quiescent zone in the flotation cell. In this method, voltage variations were measured at various heights of the cell at different impeller speeds using the piezoelectric sensor (to be introduced in the next section). Then the graph of voltage variations against the relative height of the cell was plotted, and the border between zones was identified based on the method proposed by Tabosa et al. [12].

2.2.3. Measuring turbulence

In this work, an LDTO-028 piezoelectric sensor was used to measure the turbulence, as suggested by Meng et al. [13]. The piezoelectric sensor was connected to a rod and was located in the cell inside a mesh surface (to prevent the sensor vibration) and was used to measure the turbulence at various depths (as shown in Figure 1). A filtering integrated circuit, as proposed by the sensor manufacturer, was used. Signals were transferred to a computer via a 4704 Advantech card. Finally, the analysis of the received signals was done by the Matlab Signal Processing toolbox. Using the correlation between the displacement and amplitude to frequency ratio [13], the velocity fluctuation of a certain measurement was calculated:

- (1) The signal was processed with a Fast Fourier Transform (FFT) algorithm to obtain the spectrum.
- (2) For each spectrum component, the frequency (f), amplitude (A), and displacement (D) were obtained.
- (3) $f * D$ was calculated for each frequency.
- (4) The mean velocity was calculated from these product values at different frequencies and was considered to be the representation of turbulence.

2.2.4. Measuring solid suspension

The samples were collected from three points of the quiescent zone (as shown in Figure 1) by a peristaltic pump with a constant flow rate, and the solid percentage was calculated after filtration and drying the samples. Five samples were taken from each point, and their average was used as the final solid percentage. After each test, a compensating pulp with a similar concentration was added to the

cell via the peristaltic pump to keep the experimental conditions constant.

2.2.5. Measuring gas hold-up

The gas hold-up was measured using the electrical conductivity method, where the electrical conductivity of pulp with and without air was measured, and the value of gas hold-up was calculated based on the Maxwell equation [14]:

$$\varepsilon_g = \frac{1 - \frac{k_d}{k_p}}{1 + 0.5 \frac{k_d}{k_p}} \quad (1)$$

Where k_p and k_d are defined as pulp electrical conductivity with and without air, respectively [14].

It should be mentioned that two different conductivity cells were used to measure the conductivity, a larger cell (of 5.5 cm diameter) for measuring the conductivity in the quiescent zone, and a smaller one (of 2.5 cm diameter) to measure the local conductivity. Since the inline measurement of the electrical conductivity was not constant and had minor changes, 30 datasets were read in each test, and the average of these data was recorded as the value of the electrical conductivity.

2.2.6. Modeling approach

In order to demonstrate the relationship between the impeller speed and the entrainment, the four characteristics of the quiescent zone including height, turbulence, solid percentage, and gas hold-up were measured in the flotation experiments, and an attempt was made to correlate the impeller speed and the resulting entrainment to these characteristics (Figure 2). The correlation matrix and the variance inflation factor (VIF) between the variables were calculated to examine the co-linearity between the variables. VIF is the ratio of variance in a model with multiple terms divided by the variance of a model with one term alone. It quantifies the severity of co-linearity in an ordinary least squares regression analysis [15]. The co-linearity between the variables causes an inaccurate estimation of the regression coefficients. Ridge Regression is a technique used for analyzing the multiple regression data that suffers from co-linearity. When co-linearity occurs, least squares estimates are unbiased but their variances are large so they may be far from the true value. As a result, Ridge regression was

used to build the empirical model, where the co-linearity between the variables was removed by adding a constant value, k to $[X^T X]^{-1}$. In order to obtain the suitable k , the chart of Ridge trace was plotted, as proposed by Montgomery, and the lowest possible k that stabilized the coefficients was chosen [15].

The regression coefficients were calculated using the modified $[X^T X]^{-1}$, and the entrainment was

modeled as a function of turbulence, solid percentage, and gas hold-up. Then a mathematical relation was presented between the impeller speed and each of the quiescent zone properties, and by substituting these relations in the Ridge regression model, the entrainment was modeled as a function of the impeller speed. The reason for why the height of the quiescent zone was not considered in the model will be explained in another section.

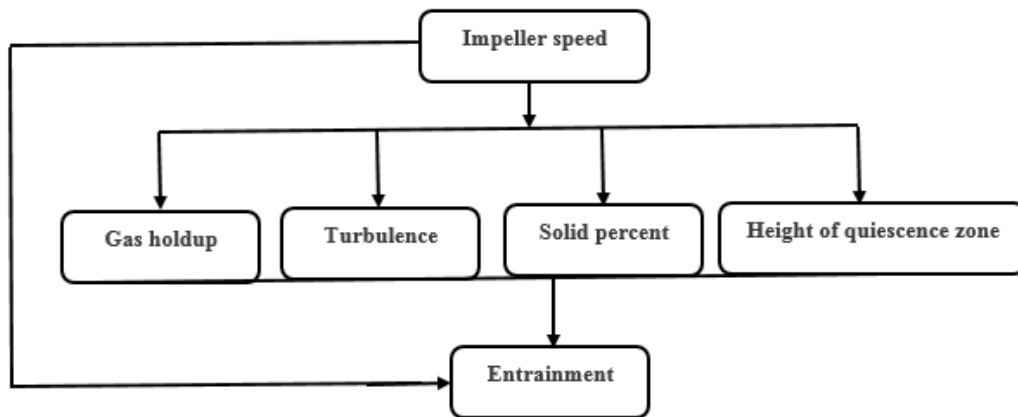


Figure 2. Relationship between variables.

3. Results and discussion

3.1. Effect of impeller speed on height of quiescent zone

As shown in Figure 3, for all impeller speeds, the maximum turbulence was observed at the relative height of 0.1, exactly where the impeller was emplaced. The turbulence value was then decreased and leveled off at a relative height of 0.3. Hence, the height of the quiescent zone was independent from the impeller speed in the conditions of these experiments so the height of quiescent zone was not considered in the model.

3.2. Effect of impeller speed on turbulence of quiescent zone

The amount of mean velocity in quiescent zone was enhanced by increasing the impeller speed, as shown in Figure 4. According to research, more turbulence under the froth-pulp interface leads to more entrainment [2], so by increasing turbulence in a higher impeller speed, more entrainment is expected to be seen, while in some studies, this trend was not observed [9, 10].

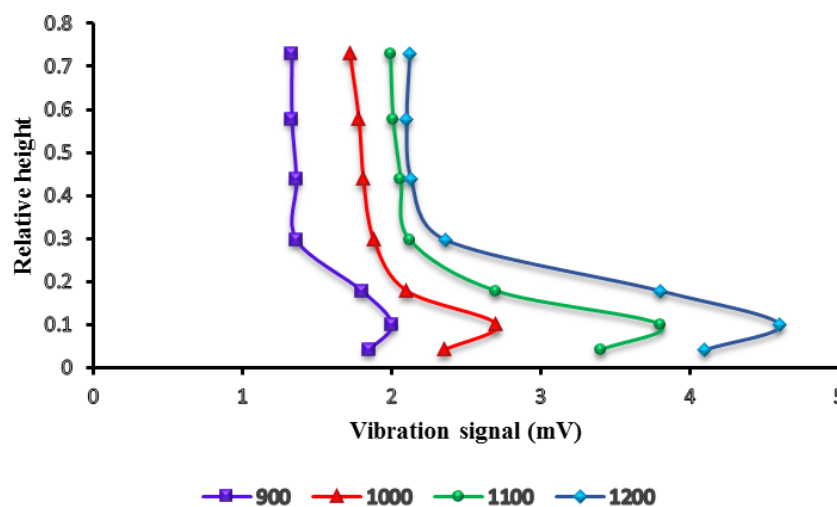


Figure 3. Relationship between impeller speed and height of quiescent zone.

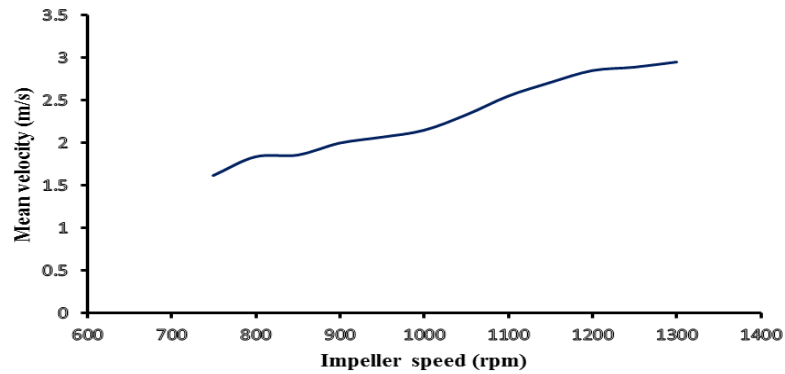


Figure 4. Effect of impeller speed on turbulence of quiescent zone.

3.3. Effect of impeller speed on suspended solids

The effect of impeller speed on suspended solids in the quiescent zone is illustrated in Figure 5 for 3 particle sizes of -50μ , $-75+50\mu$, and $-90+75\mu$.

The amount of solids in the quiescent zone was enhanced by increasing the impeller speed in case of each size fraction, while the mass of the particles less than 50μ was more than that of the other two fractions. In the pulp phase, fine particles are easily suspended in the water or the water film surrounding the bubbles in the region below the pulp/froth interface compared with coarse particles, and hence, they have more chance to travel up through the froth to the concentrate [1]. This means that by increasing the impeller speed, the available particles to occurrence of entrainment (less than 50μ) increased. Like the previous section, it is expected to see more entrainment at a higher impeller speed in this condition as well.

3.4. Effect of impeller speed on gas hold-up in quiescent zone

As the impeller speed is raised, the size of bubbles and, therefore, the rate of bubble ascent decreases,

and as a result, the gas hold-up increases [16]. However, according to Figure 6, the gas hold-up increased as the impeller speed was raised until it reached its maximum value at the impeller speed of 1100 rpm. Thereafter, the gas hold-up drastically decreased unexpectedly.

In order to be able to explain this trend, the local variations of the gas hold-up in different points of the quiescent zone were measured using the smaller measuring cell.

As it could be seen in Figure 7, the measured gas hold-up was relatively uniform at lower impeller speeds; hence, there were uniformly available bubbles for the entrainment phenomenon to occur. However, the abundance of bubbles was enhanced at higher speeds around the wall and the impeller area, leading to reduction of bubbles in the other parts of the quiescent zone. Therefore, the reduction in measured gas hold-up in Figure 6 above 1100 rpm could be attributed to the non-uniform distribution of bubbles in the quiescent zone at higher impeller speeds.

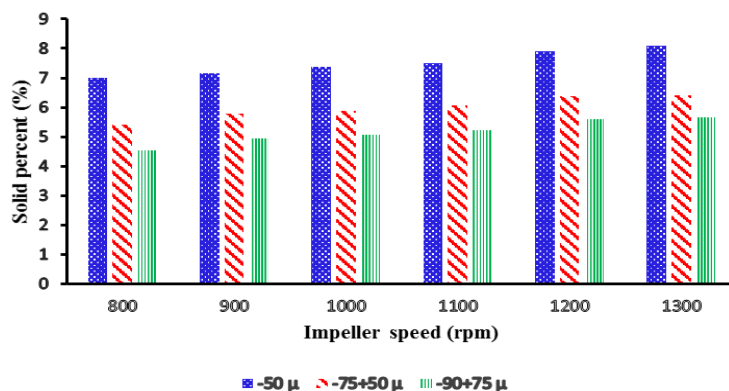


Figure 5. Effect of impeller speed on amount of transferred materials to quiescent zone in case of the three size fractions.

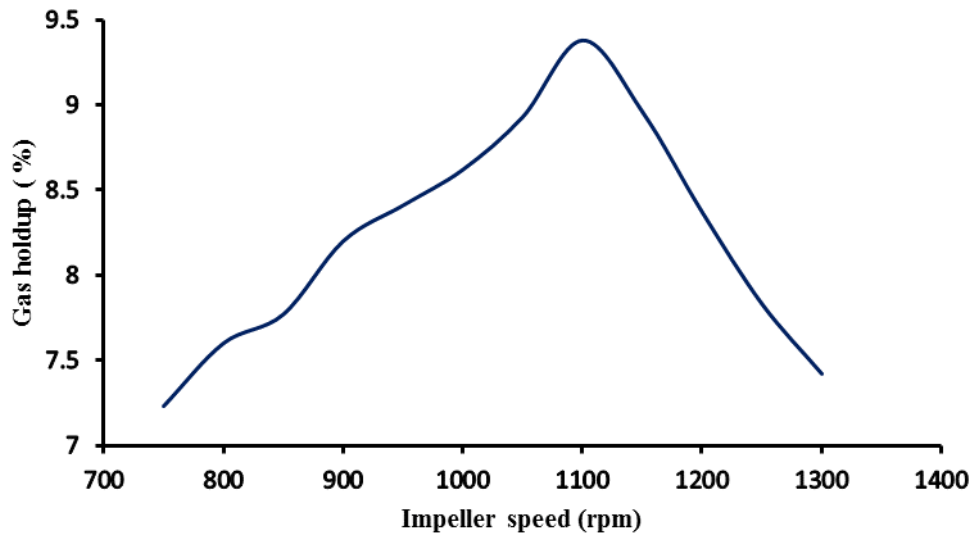


Figure 6. Effect of impeller speed on gas hold-up in quiescent zone.

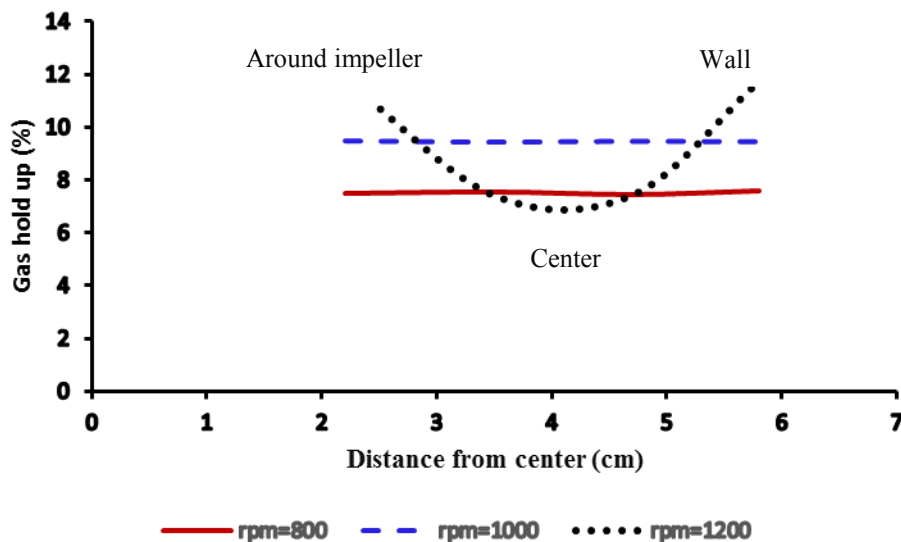


Figure 7. Local gas hold-up values measured at different distances around impeller shaft within quiescent zone for different impeller speeds.

3.5. Effect of impeller speed on entrainment

The entrainment against impeller speed is shown in Figure 8. By increasing the impeller speed, a great enhancement in entrainment was observed but at a higher impeller speed, the slope of entrainment curve was relatively constant. This trend is consistent with Yang et al. [10].

According to the bubble swarm theory, as each layer of bubbles is pushed up, another layer of bubbles will form. In this way, more solids suspended in the water are pushed up to the froth [1]; at the quiescent zone, the large population of bubbles due to increasing impeller speed led to a decrease in the drainage of solids and thus increased the entrainment. As shown in Figure 6,

at impeller speeds higher than 1100 rpm, the gas hold-up decreased, and the result was an increase in the particle drainage and a decrease in entrainment.

As a result, the trend of variation of solid percentage and turbulence by increasing impeller speed was in agreement with entrainment enhancement, while the gas hold-up caused the reduction of entrainment at higher speeds. Subsequently, a mild enhancement of entrainment at higher speeds of impeller would occur. This can substantially explain why the impeller speed and its interaction with other factors do not have a significant impact on the entrainment.

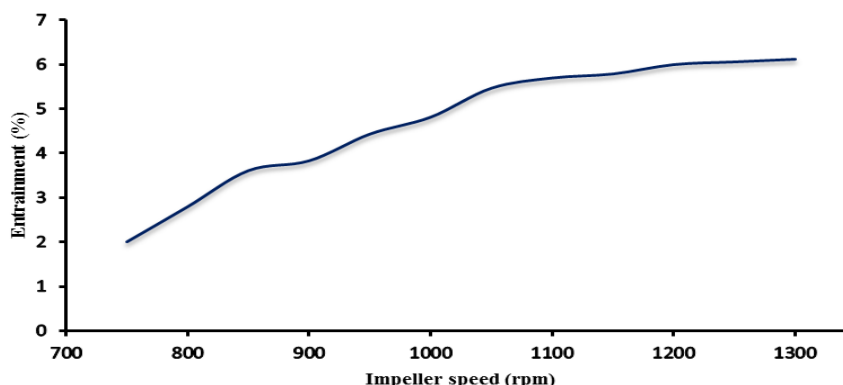


Figure 8. Relationship between entrainment and impeller speed.

3.6. Developing an empirical model

The regression method was employed to propose an empirical model to demonstrate the effect of properties of the quiescent zone on the entrainment phenomenon. According to Table 1, the data was reasonably correlative. The VIF values bigger than 10 were also indicative of the co-linearity between the variables [15].

In order to estimate the regression coefficients correctly, it is necessary to remove the co-linearity between the variables, and therefore, the Ridge regression method was applied. Based on the Ridge trace graph (Figure 9), $K = 0.293$ was selected to stabilize the coefficients.

Considering the value of $K = 0.293$, the regression coefficients were calculated, so that the entrainment was presented as a function of the solid percentage, gas hold-up, and the turbulence of the quiescent zone (Equation (2)). It is worth mentioning that this equation is only suitable for the conditions at which the independent factors (dependent on each other here) vary as a result of variation in the impeller speed.

$$R_{en} = 1.04x + 1.15v + 0.41\varepsilon_g - 8.94 \quad (2)$$

where R_{en} is the recovery by entrainment, X is the solid percentage, V is the turbulence, and ε_g is the gas hold-up.

The relationship between the predicted model and the measured data is shown in Figure 10. The error between the actual data and the model was calculated using Root-Mean-Square Error, which showed $RMSE = 0.266$, which is assumed as an acceptable value [17].

The relation between the impeller speed and the three properties of the quiescent zone were obtained by regression (Figure 11):

$$x = 0.029rpm + 4.3755 \quad (3)$$

$$v = 0.0025rpm - 0.275 \quad (4)$$

$$\varepsilon_g = -2 * 10^{-5} rpm^2 + 0.045rpm - 14.724 \quad (5)$$

The linear relationship between X and V with rpm indicates that at all conditions, by increasing the impeller speed (rpm), X and V will increase.

Equation 5 is a second-order equation, showing an upward curvature. According to Equations 3-5, the trend of entrainment variation versus rpm in empirical model presented in Equation 2 is logical as at 750-1100 rpm , X , V , and ε_g increased, and therefore, entrainment enhanced sharply. However, at a higher rpm , despite the increase in X and V , ε_g decreased. A mild enhancement of entrainment was observed for higher speeds of impeller, as suggested by Wang et al. [9] and Yang et al. [10] as well.

Finally, with the replacement of X , V , and ε_g in Equation 2 by Equations 3-5, a model describing the relationship between the impeller speed and the entrainment is presented as Equation 6.

$$R_{en} = -0.82 * 10^{-5} rpm^2 + 0.024rpm - 10.47 \quad (6)$$

It should be noted that these empirical models are valid in the range of 750-1300 rpm and in the conditions applied in the experiments. The relationship between the predicted model and the measured data are shown in Figure 12 ($RSME=201$).

Table 1. Correlation matrix and VIF between variables.

Variables	Solid percentage, X	Mean velocity, V	Gas hold-up, ε_g	VIF
Solid percentage, X	1	0.96	0.38	17.68
Mean velocity, V	0.96	1	0.29	16.45
Gas holdup, ε_g	0.38	0.29	1	1.31

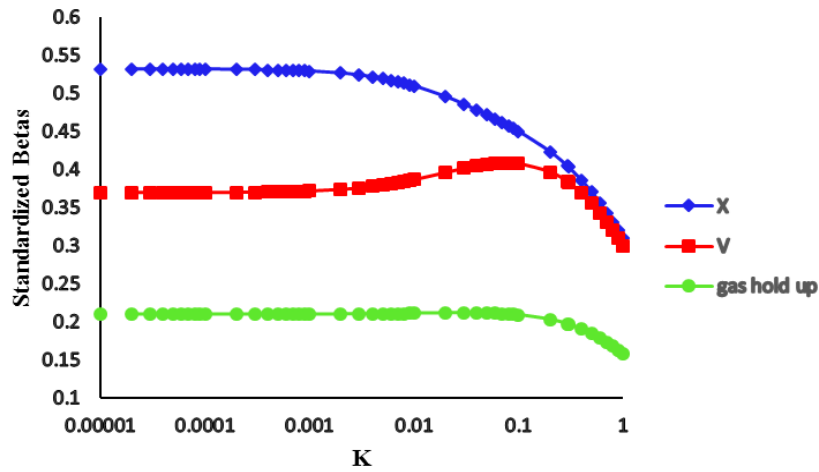


Figure 9. Graph of Ridge trace for normalized data.

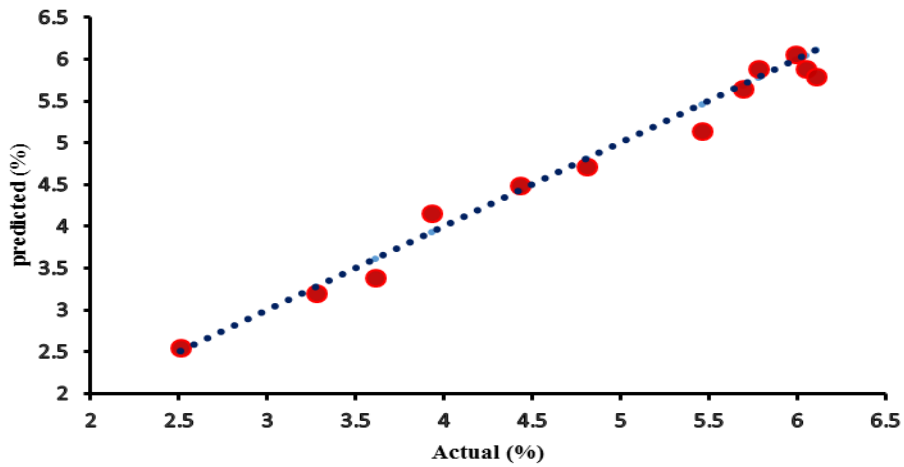


Figure 10. Predicted values against real values of entrainment.

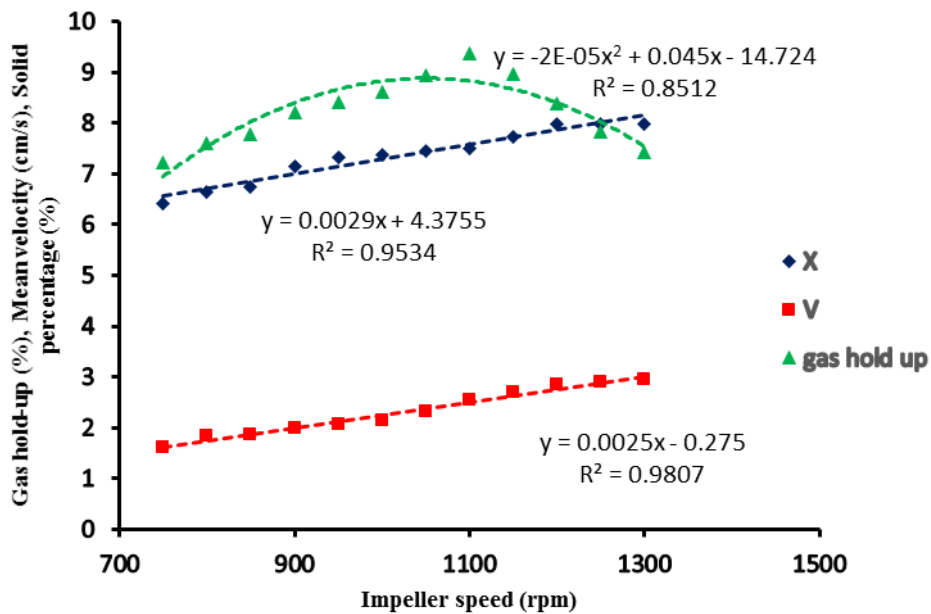


Figure 11. Relationship between impeller speed and properties of quiescent zone.

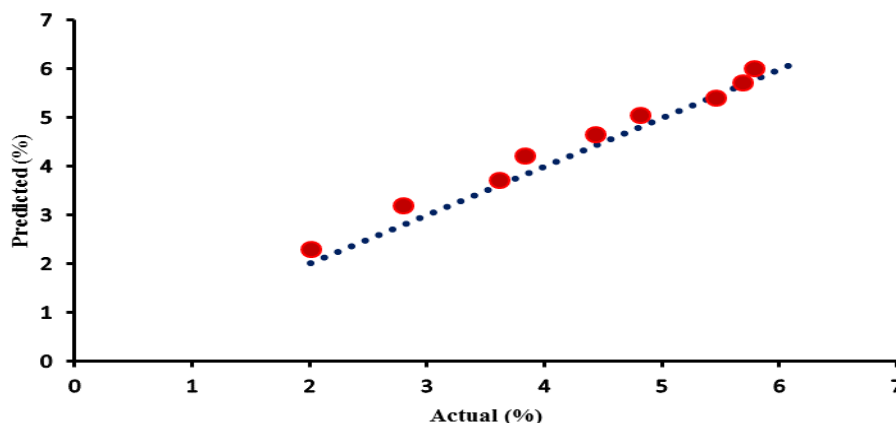


Figure 12. Predicted values against real values of entrainment.

4. Conclusions

The impact of the impeller speed on four characteristics of the quiescent zone in a laboratory flotation cell, i.e. zone height, turbulence, solid percentage, and gas hold-up, and their relationship with the entrainment was investigated. The height of the quiescent zone was found to be independent from the impeller speed variations. The turbulence value and the solid percentage in the quiescent zone were enhanced by increasing the impeller speed, while the gas hold-up was enhanced by increasing the impeller speed up to 1100 rpm, then decreased significantly as for impeller speeds above 1100 rpm. The reason for gas hold-up reduction was attributed to the variation of bubble distribution pattern within the cell. The entrainment enhanced from 2.01 to 5.69% by increasing the impeller speed from 750 to 1100 rpm but variations of the entrainment were not significant above 1100 rpm. By increasing the impeller speed, the variation of solid percentage and turbulence were in agreement with entrainment enhancement, while the gas hold-up reduction above 1100 caused a decrease in the entrainment. Generally, raising impeller speed, as long as increasing the solid percentage, turbulence, and gas hold-up, caused a drastic increase in entrainment. Despite the increase in solid percentage and turbulence, the gas hold-up decreased, and as a result, the entrainment raised with a smaller slope. This point means that bubble distribution has a key role in the entrainment phenomenon. Yet, deep knowledge of this role needs further investigations.

Acknowledgments

The Authors would like to express their sincere thanks to floatation laboratory staff of Tarbiat Modares University for their technical assistance.

References

- [1]. Wang, L., Peng, Y., Runge, K. and Bradshaw, D. (2015). A review of entrainment: Mechanisms, contributing factors and modelling in flotation. *Minerals Engineering*. 70: 77-91.
- [2]. Nguyen, A. and Schulze, H.J. (2003). *Colloidal science of flotation* (Vol. 118). CRC Press.
- [3]. Savassi, O.N. (2005). A compartment model for the mass transfer inside a conventional flotation cell. *International Journal of Mineral Processing*. 77 (2): 65-79.
- [4]. Gorain, B.K., Franzidis, J.P. and Manlapig, E.V. (2000). *Flotation Cell Design: Application of Fundamental Principles*. Julius Kruttschnitt Mineral Research Centre. Indooroopilly. Queensland. Australia.
- [5]. Schubert, H. (1999). On the turbulence-controlled micro processes in flotation machines. *International Journal of Mineral Processing*. 56 (1-4): 257-276.
- [6]. Tang, M., Wen, S. and Tong, X. (2015). Effects on entrainment of serpentines by hydrophobic flocs of ultra-fine copper-nickel sulfides during flotation. *Journal of the Southern African Institute of Mining and Metallurgy*. 115: 687-690.
- [7]. Akdemir, Ü. and Sönmez, İ. (2003). Investigation of coal and ash recovery and entrainment in flotation. *Fuel Processing Technology*. 82 (1): 1-9.
- [8]. Cilek, E.C. (2009). The effect of hydrodynamic conditions on true flotation and entrainment in flotation of a complex sulfide ore. *International Journal of Mineral Processing*. 90 (1-4): 35-44.
- [9]. Wang, L., Peng, Y. and Runge, K. (2016). Entrainment in froth flotation: The degree of entrainment and its contributing factors. *Powder Technology*. 288: 202-211.
- [10]. Yang, X.S. and Aldrich, C. (2006). Effects of impeller speed and aeration rate on flotation performance of sulfide ore. *Transactions of Nonferrous Metals Society of China*. 16 (1): 185-190.

[11]. Trahar, W.J. (1981). A rational interpretation of the role of particle size in flotation. *International Journal of Mineral Processing*. 8 (4): 289-327.

[12]. Tabosa, E., Runge, K., Holtham, P. and Duffy, K. (2016). Improving flotation energy efficiency by optimizing cell hydrodynamics. *Minerals Engineering*. 96: 194-202.

[13]. Meng, J., Xie, W., Brennan, M., Runge, K. and Bradshaw, D. (2014). Measuring turbulence in a flotation cell using the piezoelectric sensor. *Minerals Engineering*. 66: 84-93.

[14]. Sanwani, E., et al. (2006). Comparison of gas hold-up distribution measurement in a flotation cell using capturing and conductivity techniques. *Minerals Engineering*. 19(13): 1362-1372.

Sanwani, E., Zhu, Y., Franzidis, J.P., Manlapig, E.V. and Wu, J. (2006). Comparison of gas hold-up

distribution measurement in a flotation cell using capturing and conductivity techniques. *Minerals engineering*. 19 (13): 1362-1372.

[15]. Douglas, C.M. and George, C.R. (2003). *Applied statistics and probability for engineers*. John Wiley & Sons, Inc. 605: 506-564.

[16]. Sovechles, J.M., Lepage, M.R., Johnson, B. and Waters, K.E. (2016). Effect of gas rate and impeller speed on bubble size in frother-electrolyte solutions. *Minerals Engineering*. 99: 133-141.

[17]. Veerasamy, R., Rajak, H., Jain, A., Sivadasan, S., Varghese, C.P. and Agrawal, R.K. (2011). Validation of QSAR models-strategies and importance. *International Journal of Drug Design & Discovery*. 3: 511-519.

اثر دور همزن بر خواص ناحیه راکد و ارتباط آن با دنباله‌روی در سلول فلوتاسیون مکانیکی

سیما رزمجویی، محمود عبدالمهی* و محمدرضا خالصی

بخش مهندسی معدن، دانشکده فنی مهندسی، دانشگاه تربیت مدرس، ایران

ارسال ۲۰۱۸/۰۱/۰۶، پذیرش ۲۰۱۸/۰۲/۱۵

* نویسنده مسئول مکاتبات: minmabd@modares.ac.ir

چکیده:

در سلول‌های فلوتاسیون مکانیکی، آشفتگی یک عامل بسیار تأثیرگذار است. در این پژوهش، اثر دور همزن بر چهار ویژگی ناحیه راکد یعنی ارتفاع ناحیه راکد، درصد جامد، آشفتگی و ماندگی گاز بررسی و در نهایت ارتباط آن‌ها با دنباله‌روی مطالعه شد و نشان داده شد که چرا در دوره‌های بالای همزن، تغییرات دنباله‌روی ناچیز است. آشفتگی و درصد جامد به ترتیب با استفاده از سنسور پیزوالکتریک و پمپ پرستالیتیک انجام شد و برای اندازه‌گیری ماندگی گاز از روش هدایت الکتریکی استفاده شد. طبق نتایج، با افزایش دور همزن از ۷۵۰ تا ۱۱۰۰ دور بر دقیقه، مقدار دنباله‌روی از ۲/۰۱ تا ۵/۶۹ تغییر کرد ولی در دوره‌های بالاتر از ۱۱۰۰ دور بر دقیقه، تغییرات محسوسی دیده نشد. ارتفاع ناحیه راکد مستقل از تغییرات دور همزن بود در حالی که درصد جامد، آشفتگی و ماندگی گاز در این محدوده (۷۵۰-۱۱۰۰) افزایش یافت و علیرغم افزایش درصد جامد و آشفتگی در دوره‌های بالاتر از ۱۱۰۰ دور بر دقیقه، ماندگی گاز کاهش یافت؛ بنابراین کاهش ماندگی گاز در دوره‌های بالاتر را می‌توان عامل تغییرات کم دنباله‌روی در دوره‌های بالاتر از ۱۱۰۰ دور بر دقیقه دانست. علت کاهش ماندگی گاز تغییر الگوی توزیع حباب بود. در ادامه با استفاده از روش رگرسیون ریج، مدلی برای نشان دادن ارتباط بین دنباله‌روی و خواص ناحیه راکد ارائه شد.

کلمات کلیدی: دور همزن، آشفتگی، ناحیه راکد، دنباله‌روی، سلول فلوتاسیون مکانیکی.
